·脊柱脊髓疾病·

脊髓空洞症大鼠模型长期稳定性评价

姚庆宇 马龙冰 菅凤增

【摘要】 **目的** 探讨硬脊膜外压迫法构建脊髓空洞症大鼠模型的长期稳定性。**方法** 共35只Sprague-Danley大鼠随机分为假手术组(9只)、短期实验组(6只)和长期实验组(20只),硬脊膜外压迫法阻塞脊髓中央管以诱导脊髓空洞形成,分别于术前及术后3、6、9和12个月采用Basso-Beattie-Bresnahan评分(BBB)评估后肢运动功能;术后2和12个月行MRI检查和HE染色评估脊髓空洞形态学改变。**结果** 术后2和12个月时,MRI检查显示长期实验组分别有80%(16/20)和85%(17/20)大鼠出现脊髓空洞;与术后2个月相比,长期实验组大鼠术后12个月时最大空洞前后径与其所在脊髓平面前后径比值($Z=-3.518$,$P=0.000$)和最大空洞面积与其所在脊髓平面面积比值($Z=-3.464$,$P=0.001$)均增加;假手术组大鼠术后2和12个月时脊髓形态正常、无空洞形成,术后2个月时短期实验组可见脊髓空洞形成,术后12个月时长期实验组空洞面积不仅大于短期实验组且累及更多椎体节段;假手术组和长期实验组大鼠手术前后不同时间点BBB评分差异无统计学意义(均$P>0.05$)。**结论** 硬脊膜外压迫法构建脊髓空洞症大鼠模型阳性率高,具有较好的长期稳定性,且不影响运动功能。

【关键词】 脊髓空洞症; 硬膜外隙; 磁共振成像; 病理学; 疾病模型,动物

Long-term stability evaluation of syringomyelia rats

YAO Qing-yu, MA Long-bing, JIAN Feng-zeng

Department of Neurosurgery, Xuanwu Hospital, Capital Medical University, Beijing 100053, China

Corresponding author: JIAN Feng-zeng (Email: jianfengzeng@xwh.ccmu.edu.cn)

【**Abstract**】 **Objective** To investigate the long-term stability of syringomyelia (SM) rat model constructed by epidural compression. **Methods** A total of 35 Sprague-Danley (SD) rats were randomly divided into sham surgery group (n = 9), short-term group (n = 6) and long-term group (n = 20). The central spinal canal was blocked by epidural compression to induce SM in rats. Basso-Beattie-Bresnahan score (BBB) was used to evaluate lower limb motor function before surgery and at 3, 6, 9 and 12 months after surgery. The morphological changes of SM were evaluated by MRI and HE staining at 2 and 12 months after surgery. **Results** At 2 and 12 months after surgery, MRI showed 80% (16/20) and 85% (17/20) rats in long-term group had SM. Compared with 2 months after surgery, the ratio of the maximum cavity diameter to the diameter of spinal cord plane ($Z=-3.518$, $P=0.000$) and the ratio of the maximum cavity area to the area of spinal cord plane ($Z=-3.464$, $P=0.001$) increased in long-term group at 12 months after surgery. At 2 and 12 months after surgery, the morphology of the spinal cord was normal and there was no cavity in sham surgery group, while the spinal cord cavity was observed in the short-term group at 2 months after surgery. At 12 months after surgery, the cavity area of the long-term group was not only larger than that of the short-term group, but also involved more vertebral segments. There was no significant difference in BBB score between sham surgery group and long-term group at different time points before and after surgery ($P>0.05$, for all). **Conclusions** The rat model of SM constructed by epidural compression has high positive rate, good long-term stability, and does not affect the motor function of rats.

【**Key words**】 Syringomyelia; Epidural space; Magnetic resonance imaging; Pathology; Disease models, animal

This study was supported by China Postdoctoral Science Fundation Funded Project (No. 2018M641412).

Conflicts of interest: none declared

doi:10.3969/j.issn.1672-6731.2022.08.003

基金项目:中国博士后科学基金资助项目(项目编号:2018M641412)

作者单位:100053 北京,首都医科大学宣武医院神经外科

通讯作者:菅凤增,Email:jianfengzeng@xwh.ccmu.edu.cn

脊髓空洞症(SM)是一种慢性进行性脊髓变性疾病,以脊髓内充满脑脊液的异常空洞为特征,常继发于Chiari畸形(CM)、髓内肿瘤或脊髓损伤(SCI)等脊髓病变[1-6]。临床表现主要包括肢体疼痛、节段性分离性感觉障碍、肢体运动障碍、肌无力和肌萎缩等[7-10]。一般而言,脊髓空洞症患者就诊时神经系统已出现不可逆性损伤,治疗效果及预后欠佳[7]。动物模型是研究脊髓空洞症相关病理生理学机制的基础,而模型的长期稳定性则是机制研究获益的重要前提,目前实验室较为常用的动物模型以高岭土或使君子酸构建的脊髓空洞症大鼠模型为主,但这两种物质在形成脊髓空洞症的同时可诱发脊髓炎和继发性脊髓损伤[11-13]。我们课题组在前期研究中采用硬脊膜外压迫法成功构建一种新型脊髓空洞症大鼠模型,不仅规避传统建模方法诱发炎症和感染风险,而且具有较好的短期稳定性[14]。为进一步明确该模型的长期特性,本研究通过硬脊膜外压迫法构建脊髓空洞症大鼠模型并观察其长期稳定性,以探究脊髓空洞症发生发展进程。

材料与方法

一、实验材料

1.实验动物与分组 清洁级健康8周龄雌性Sprague-Dawley(SD)大鼠共35只,体重250~300 g,购自北京维通利华实验动物技术有限公司[许可证号:SYXK(京)2017-0033]。于室温(20±2)℃、相对湿度50%~60%、12 h昼-12 h夜循环照明环境中自由摄食、饮水,适应性饲养3 d后进行动物实验。根据随机数字表法,将35只大鼠随机分为假手术组(9只)、短期实验组(6只)和长期实验组(20只)。

2.药品与仪器 (1)药品与试剂:头孢呋辛钠(纯度100%,规格0.25 g)购自中国国药集团志军制药有限公司,恩氟烷(纯度100%,规格150 ml)为河北一品制药有限公司产品,戊巴比妥钠(纯度99.99%,规格5 g)由上海思域化工科技有限公司提供。(2)仪器与设备:Pharma Scan 7.0T MRI扫描仪、OPMI Pico手术显微镜和DM750生物学显微镜分别为德国Bruker Corp公司、Carl Zeiss公司及Leica公司产品;LOGAN 3×3显微撑开器购自深圳瑞沃德生命科技有限公司。

二、实验方法

1.模型制备 大鼠俯卧位,呼吸面罩吸入麻醉(2%恩氟烷,70%一氧化二氮,30%氧气)。根据$T_{9\sim11}$椎体连接紧密且融为一体、T_8与T_9椎体之间存在相对宽大空隙等特点,先定位T_8椎体,然后基于T_8与$T_{9\sim11}$椎体之间的相对位置关系,依次向下定位至T_{13}椎体;以T_{13}椎体为中心,行3 cm皮肤切口。于手术显微镜下微型牵开器牵开T_{12}-L_1椎旁肌,显露T_{12-13}椎间隙之间的黄韧带,显微剪做3~4 cm切口,以避免脑脊液漏和非压迫部位硬脊膜塌陷,以确保硬脊膜完整[14]。将1.50 mg无菌棉球塑型成长条状,并用显微神经剥离子缓慢塞入T_{13}椎板下方的硬脊膜外间隙,通过椎间隙见硬脊膜明显下陷且贴合脊髓表面,即为脊髓中央管阻塞成功(图1)。假手术组大鼠仅切开皮肤、显露肌肉、切开黄韧带,不行硬脊膜外压迫。手术结束以生理盐水冲洗术区和皮下间隙,逐层缝合肌肉和皮肤;术后每8小时腹腔注射头孢呋辛钠100 mg/kg预防感染,持续1周。短期实验组和长期实验组大鼠中央管阻塞成功率为100%(26/26),术后MRI或HE染色显示脊髓中央管空洞形成,即脊髓空洞症模型构建成功。

2.运动功能评价 采用Basso-Beattie-Bresnahan评分(BBB)[15]于术前1周及术后3、6、9和12个月时对假手术组和长期实验组大鼠进行后肢运动功能评价,两组完成测量的动物数分别为假手术组6只(其余3只于术后2个月处死行组织学形态观察)、长期实验组20只。评价维度包括关节活动度、肌肉收缩力、步态稳定性、肢体协调性、负重能力和精细运动共计6项,总评分为21分,0~7分为重度损伤,负重能力差,无关节屈曲,或有关节屈曲但仅可在地面拖行;8~13分为中度损伤,负重能力略高于重度损伤,具备一定协调运动能力,但仍存在关节僵硬;14~21分为轻度损伤,负重能力略高于中度损伤,前后肢运动协调,仅有轻微运动障碍。

3.空洞形态评价 采用Pharma Scan 7.0T MRI扫描仪,分别于术后2个月(假手术组9只、长期实验组20只)和12个月(假手术组6只、长期实验组20只)对大鼠进行MRI扫描,以术区为中心,单通道头部线圈,梯度场强400 mT/m,扫描序列T_2-RARE。(1)横断面扫描参数:重复时间(TR)4500 ms、回波时间(TE)33 ms,翻转角(FA)90°,扫描视野(FOV)60 mm×40 mm,矩阵为256×256,激励次数(NEX)为8次,层厚1 mm、层间距为零,共扫描30层,扫描时间720 s。(2)矢状位扫描参数:重复时间3000 ms、回波时间33 ms,翻转角为90°,扫描视野为60 mm×40 mm,矩阵256×256,激励次数为8次,层厚为

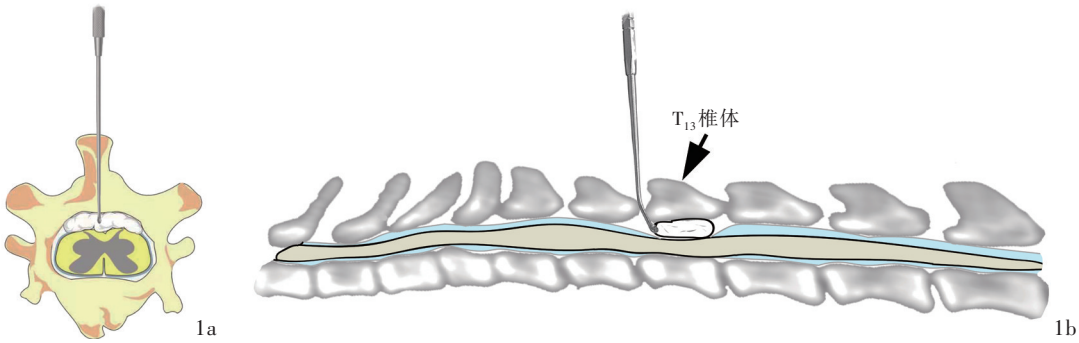

图1 脊髓空洞症模型制备方法示意图：于T_{12-13}椎间隙切开黄韧带，将1.50 mg长条状棉条塞入T_{13}椎板下方的硬脊膜外间隙，以阻止脑脊液流动 1a 水平面观 1b 矢状面观

Figure 1 Schematic diagram of the syringomyelia model: the ligamentum flavum was cut in the lamina space of T_{12-13}, and a 1.50 mg long-strip of cotton was inserted into the epidural space below the lamina of T_{13} to prevent the flow of cerebrospinal fluid. Horizontal plane view (Panel 1a). Sagittal plane view (Panel 1b).

0.60 mm、层间距为零，共扫描10层，扫描时间为720 s。扫描结束后将T_2WI图像导入Radiant软件（https://www.radiantviewer.cn），脊髓空洞区域呈白色高信号，边缘清晰。采用Radiant软件“直线测量工具”和“面积测量工具”分别测量最大空洞前后径（n）及其面积（S_1），以及空洞所在脊髓平面前后径（m）及其面积（S_2），计算直径比（n/m）和面积比（S_1/S_2），以评价脊髓空洞扩张情况（图2）。

4. 术后脊髓组织学形态观察 于术后2个月（假手术组3只、短期实验组6只）和12个月（假手术组6只、长期实验组20只）进行组织学形态观察。采用戊巴比妥钠（150 mg/kg）麻醉后打开胸腔、显露心脏，0.01 mol/L磷酸盐缓冲盐液、质量分数为4%多聚甲醛溶液经左心室灌注处死大鼠，剥离脊髓，4%多聚甲醛溶液固定24 h，梯度乙醇脱水，制备层厚3 μm石蜡切片，行常规HE染色。

三、统计分析方法

采用SPSS 22.0统计软件进行数据处理与分析。计数资料以相对数构成比（%）或率（%）表示，采用配对χ^2检验。正态性检验采用Shapiro-Wilk检验，呈正态分布的计量资料以均数±标准差（$\bar{x} \pm s$）表示，采用前后测量设计的方差分析；呈非正态分布的计量资料以中位数和四分位间距[$M(P_{25}, P_{75})$]表示，采用Wilcoxon符号秩和检验。以$P \leqslant 0.05$为差异具有统计学意义。

结 果

本研究入组大鼠无术后瘫痪或死亡。术后2个月，假手术组大鼠脊髓形态正常、无空洞形成（图3a）；长期实验组16只大鼠[80%（16/20）]出现脊髓空洞，其中14只空洞形态呈“串珠”样，位于受压部位头侧中央管，累及2～3个椎体节段（图3b），其余2只空洞形态呈“单球”样，分别位于T_{10}和T_{11}椎体。术后12个月，假手术组大鼠脊髓形态正常、无空洞形成（图3c），长期实验组17只大鼠[85%（17/20）]出现脊髓空洞（图3d）。术后2个月与12个月长期实验组大鼠脊髓空洞阳性率差异无统计学意义（$P > 0.05$，表1），表明脊髓空洞症模型稳定性良好。长期实验组大鼠术后12个月n/m值和S_1/S_2值均高于术后2个月（$P = 0.000$，表2），表明脊髓空洞可随硬脊膜外压迫时间的延长而逐渐扩张。

HE染色显示，假手术组大鼠术后2和12个月时脊髓形态正常，无空洞形成（图4a，4b）；短期实验组大鼠术后2个月时脊髓呈“串珠”样改变，脊髓空洞形成（图4c）；长期实验组大鼠术后12个月时脊髓呈“串珠”样改变，空洞形成，且空洞面积大于短期实验组，累及更多椎体节段（图4d）。

运动功能评价显示，假手术组术前及术后3、6、9和12个月时BBB评分均为21分，长期实验组大鼠术后3个月时BBB评分为（20.81±0.40）分，其余各时间点均为21分，两组手术前后BBB评分差异无统计学意义（$P > 0.05$；表3，4），表明脊髓空洞症模型对大鼠后肢运动功能无影响。

讨 论

脊髓空洞症全球患病率为2/10万～8/10万[16]，平均发病年龄为30～40岁，病程进展缓慢[17-18]，脊髓损伤、肿瘤、先天性畸形等均可导致脊髓中央管

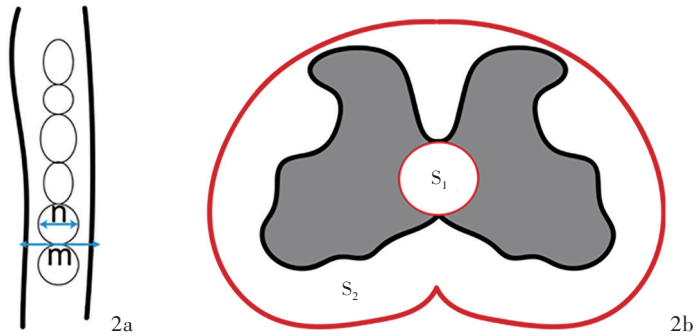

n:脊髓空洞前后径;S_1:脊髓空洞面积;m:空洞所在脊髓平面前后径;S_2:空洞所在脊髓平面面积

图2 脊髓空洞扩张示意图 2a 正中矢状面观 2b 水平面观

Figure 2 Schematic diagram of syringomyelia Median sagittal plane view (Panel 2a). Horizontal plane view (Panel 2b).

和蛛网膜下腔之间脑脊液交换失衡,从而诱发脊髓空洞症[19-21]。痛温觉分离、肢体无力、肢体瘫痪和排汗异常等神经系统症状通常在脊髓空洞症形成数年后方出现,且可持续数十年甚至终身[15]。因此,如果能够较好地模拟脊髓空洞症的发生发展过程,所构建的脊髓空洞症动物模型必须具备良好的长期稳定性,方能覆盖模式生物的全生命周期。既往对于脊髓空洞症模型大鼠的观察周期通常为3周至3个月[13,22-23],发病3个月以上的转归鲜有报道。研究显示,12月龄大鼠约相当于30岁成人[24],因此有必要对大鼠进行长达1年的随访,以观察脊髓空洞症的发生发展进程。

本研究构建的脊髓空洞症模型不与第四脑室相通,其形态模式类似Chiari畸形Ⅰ型引起的脊髓空洞症,属于非交通性脊髓空洞症,主要累及中央管,后者为一潜在性腔隙,脑脊液可在中央管与蛛网膜下腔之间自由出入且呈动态平衡,从而维持机体稳态。小脑扁桃体下疝畸形、颅底凹陷合并寰枢椎脱位、脊髓血管畸形等导致的脑脊液交换通道受阻或脊髓损伤、手术诱发的蛛网膜下腔粘连引起的脑脊液循环梗阻等均可导致脑脊液交换失衡。基于上述病因学机制,本研究采用硬脊膜外压迫法构建脑脊液循环梗阻模型[13]。正常情况下,脑脊液会随动脉搏动而产生周期性搏动,脑脊液循环梗阻时脑脊液流出受阻,但脑脊液产生未受影响,在周期性动脉搏动推动下,蛛网膜下腔的脑脊液通过血管周围间隙向脊髓实质内流动[25],这种脑脊液跨域流动以及脑脊液交换失衡[13,19,26-28]、内皮细胞连接异常、神经胶质细胞对脑脊液流量控制失衡均可导致血-脊髓屏障功能障碍[11,29],使脊髓中央管脑脊液逐渐积聚,进而形成空洞。本研究术后2个月时长期实验组有80%(16/20)大鼠出现脊髓空洞,空洞出现时间较早,利于后期长时间观察,且所有空洞均位于压迫部位的头侧,推测可能由于硬脊膜外压迫导致压迫部位头侧的蛛网膜下腔压力升高,使脑脊液跨越脊髓实质积聚于中央管而形成空洞[19]。

既往研究大多采用脊髓实质内或蛛网下腔注射高岭土或使君子酸诱导脊髓空洞产生,其原理系上述两种物质可以诱发蛛网膜炎症,使蛛网膜发生粘连,导致蛛网膜下腔梗阻、脑脊液循环梗阻、硬脊膜下腔局部压力升高,从而诱发脑脊液从高压区跨脊髓实质向低压区流动,最终形成脊髓空洞[30-31]。但高岭土或使君子酸可在硬脊膜外隙、硬脊膜下腔和脊髓实质中自由扩散,进而导致广泛的炎症和粘连[22,32]。本研究采用的硬脊膜外压迫物仅局限于T_{13}椎板下,可避免诱发弥漫性炎症。此外,我们课题组前期研究发现,采用硬脊膜外压迫法构建的脊髓空洞症模型大鼠,其硬脊膜未见胶质瘢痕增生,且脊髓实质无免疫相关小胶质细胞增生[14]。本研究结果显示,长期实验组与假手术组大鼠BBB评分差异无统计学意义,即运动功能保留率高,与注射高岭土、全横断脊髓等创伤性脊髓空洞症模型相比,该模型在模拟脑脊液动力学紊乱的同时可显著降低异物对硬脊膜下脑脊液环境造成的炎性浸润。

中央管扩张可使中央管周围灰质中的中间神经元受压,使其神经信号转导受到一定程度阻碍,主要包括痛觉、温度觉、触觉等[33-35]。本研究中大鼠横断面和矢状位MRI图像,以及横向和纵向组织切片可以从不同角度观察脊髓空洞对中央管的影响。有研究显示,脊髓空洞症动物模型中最大空洞的直径可以较好地预测脊柱疼痛、脊柱侧弯和步态异常程度[36]。本研究遵照既往研究惯例,采用MRI测量最大空洞相关数据[22,37],且为进一步消除大鼠间的个体差异,采用归一化方法,即计算脊髓空洞与其

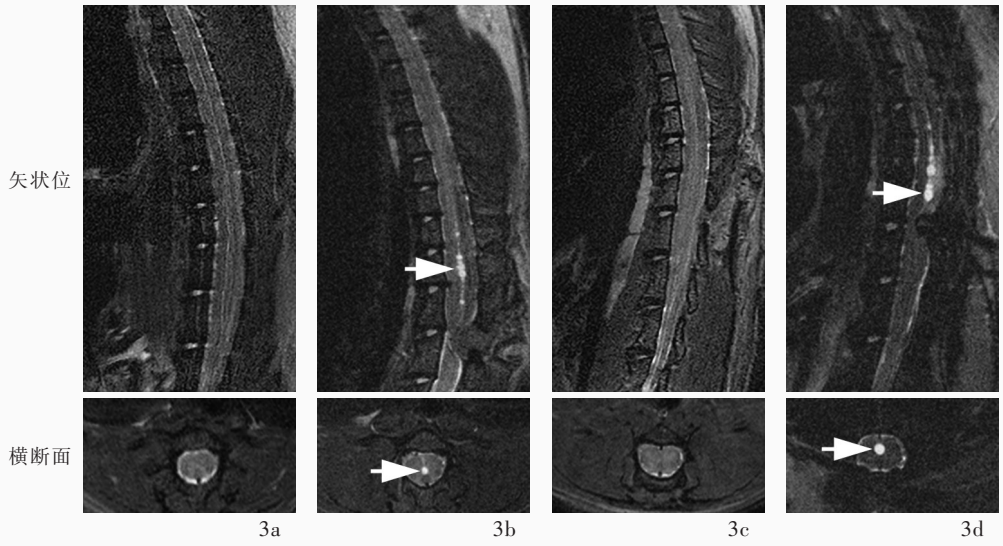

图3 矢状位和横断面脊柱T_2-RARE序列所见 3a 假手术组大鼠术后2个月时未见脊髓空洞形成 3b 长期实验组大鼠术后2个月时脊髓空洞形成(箭头所示) 3c 假手术组大鼠术后12个月时未见脊髓空洞形成 3d 长期实验组大鼠术后12个月时可见脊髓空洞,且空洞面积较术后2个月扩大(箭头所示)

Figure 3 Sagittal and axial T_2-RARE findings Syringomyelia was not observed in sham surgery group at 2 months after surgery (Panel 3a). Syringomyelia was observed in long-term group at 2 months after surgery (arrows indicate, Panel 3b). Syringomyelia was not observed in sham surgery group at 12 months after surgery (Panel 3c). Syringomyelia was observed in long-term group at 12 months after surgery, and the area of syringomyelia was larger than that at 2 months after surgery (arrows indicate, Panel 3d).

表1 长期实验组大鼠术后不同时间点脊髓空洞症阳性率的比较(例)

Table 1. Comparison of syringomyelia positive rate of long-term group in 2 and 12 months after surgery (case)

术后2个月	术后12个月		
	阳性	阴性	合计
阳性	16(16/20)	0(0/20)	16(16/20)
阴性	1(1/20)	3(3/20)	4(4/20)
合计	17(17/20)	3(3/20)	20(20/20)

*paired χ^2 test: $P=1.000$,配对χ^2检验:$P=1.000$

表2 长期实验组大鼠术后不同时间点脊髓空洞扩张程度的比较[$M(P_{25},P_{75})$]

Table 2. Comparison of dilation of syringomyelia in the long-term group in 2 and 12 months after surgery [$M\ (P_{25},\ P_{75})$]

术后观察时间	只数	n/m	S_1/S_2
2个月	16	0.22(0.11,0.26)	0.04(0.01,0.08)
12个月	16	0.23(0.12,0.27)	0.04(0.02,0.08)
Z值		-3.518	-3.464
P值		0.000	0.001

所在平面脊髓的直径比和面积比,以增强数据的同质性。此外,本研究还设置短期实验组以制备组织切片,从组织学角度观察脊髓空洞形态及位置,与MRI结果相互印证。

本研究构建的脊髓空洞症大鼠模型稳定性良好的原因可能与以下因素有关:(1)进行硬脊膜外压迫的时间适宜,本研究选择的大鼠均为8周龄,脊髓空洞症诱导4周后椎管骨性结构已达到骨骼成熟阶段[38],此时压迫物与椎管容积相对稳定,不会出现椎管生长导致压迫物相对变小的情况。(2)压迫物理化性质稳定,椎管内的非吸收性棉团持续存在,可以确保持续脑脊液循环梗阻。(3)硬脊膜外压迫物侵袭性小,棉团质地柔软,不会损伤硬脊膜和脊髓,完整的硬脊膜可以保证蛛网膜下腔静水压和渗透压梯度稳定,且可避免脊髓炎症,诱导非交通性脊髓空洞症。

手术是脊髓空洞症的主要治疗手段,根据不同病因采取不同手术方案。对于Chiari Ⅰ型畸形合并小脑扁桃体下疝所导致的脊髓空洞症,通常采用后颅窝减压术、硬脊膜扩大成形术和小脑扁桃体部分切除术;对于无小脑扁桃体下疝的脊髓空洞症,则以空洞分流术为主。脊髓空洞症导致的神经损伤具有不可逆性,虽然部分患者经手术治疗后空洞体积可部分缩小,但感觉功能无法完全恢复[39],故早期发现并及时治疗至关重要。

本研究存在以下局限性:(1)离子通道和水通

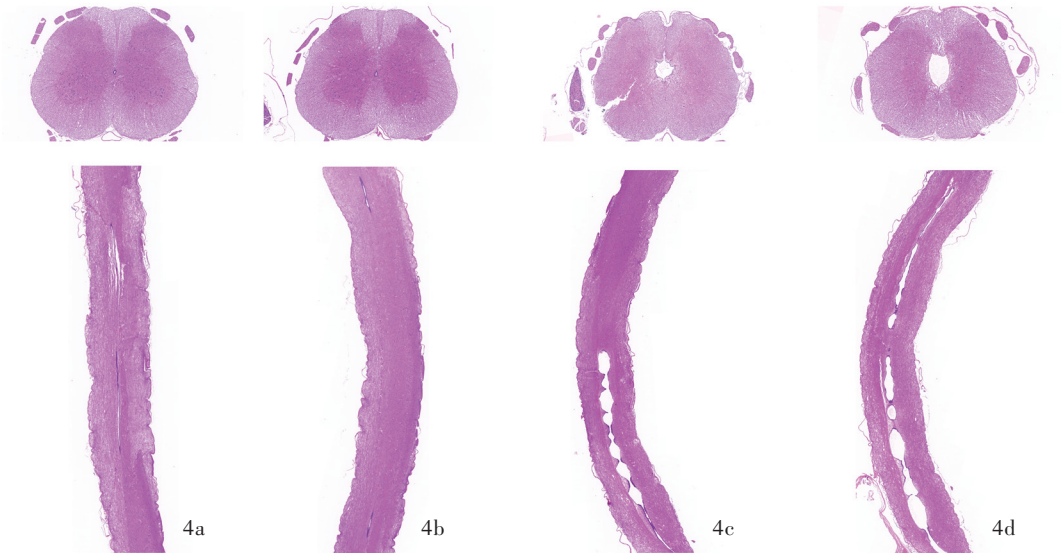

图4　术后脊髓空洞形态学改变　HE染色　低倍放大　4a　假手术组大鼠术后2个月时无脊髓空洞形成且无中央管扩张　4b　假手术组大鼠术后12个月时无脊髓空洞形成且无中央管扩张　4c　短期实验组大鼠术后2个月时可见脊髓中央管内"串珠"样改变、空洞形成　4d　长期实验组大鼠术后12个月时可见脊髓中央管内"串珠"样改变、空洞形成，且扩张程度较短期实验组明显

Figure 4　Morphological changes of syringomyelia after surgery　HE staining　Low power magnified　There was no syringomyelia formation and central canal dilation in sham surgery group at 2 and 12 months after surgery (Panel 4a, 4b). Beaded changes and cavity formation were observed in the central spinal cord in short-term group at 2 months after surgery (Panel 4c). Beaded changes and cavity formation were observed in the central spinal canal in long-term group at 12 months after surgery, and the degree of dilation was more obvious than that in short-term group (Panel 4d).

表3　假手术组与长期实验组大鼠手术前后BBB评分的比较($\bar{x}\pm s$，评分)

Table 3.　Comparison of BBB score of lower limb motor function in sham surgery group and long-term group before and after surgery ($\bar{x}\pm s$, score)

组别	只数	术前	术后3个月
假手术组	6	21.00±0.00	21.00±0.00
长期实验组	16*	21.00±0.00	20.81±0.40

*Only 16 syringomyelia positive rats were evaluated for lower limb motor function，仅对16只脊髓空洞症阳性大鼠进行后肢运动功能评价

表4　假手术组与长期实验组大鼠手术前后BBB评分的前后测量设计的方差分析表

Table 4.　ANOVA for pretest-postest measurement design of BBB score in sham surgery group and long-term group

变异来源	*SS*	df	*MS*	*F*值	*P*值
处理因素	0.077	1	0.077	1.259	0.275
测量时间	0.077	1	0.077	1.259	0.275
处理因素×测量时间	0.077	1	0.077	1.259	0.275
组间误差	1.219	20	0.061		
组内误差	1.219	20	0.061		

道蛋白在脑脊液的跨脊髓实质流动中发挥重要作用[12,40]，硬脊膜外压迫是否改变通道蛋白的表达尚待进一步研究。(2)由于脊髓空洞在后期(术后2~10个月)的进展速度较慢，本研究并未使用等距的时间节点观察其形态变化，未来将增加更多时间点，以观察脊髓空洞随时间变化的趋势。

综上所述，本研究采用硬脊膜外压迫法构建脊髓空洞症大鼠模型以观察模型的长期特性，发现该方法构建的动物模型脊髓空洞阳性率高，可避免广泛炎症和运动障碍，且脊髓空洞位于脊髓中央管，与人类脊髓空洞症的形态学特征较为接近[14]，可为探索脊髓空洞症新的治疗方案提供参考。

利益冲突　无

参　考　文　献

[1] Moriwaka F, Tashiro K, Tachibana S, Yada K. Epidemiology of syringomyelia in Japan: the nationwide survey [J]. Rinsho Shinkeigaku, 1995, 35:1395-1397.

[2] Milhorat TH, Johnson RW, Milhorat RH, Capocelli AL Jr, Pevsner PH. Clinicopathological correlations in syringomyelia using axial magnetic resonance imaging [J]. Neurosurgery, 1995, 37:206-213.

[3] Giner J, Pérez López C, Hernández B, Gómez de la Riva Á, Isla A, Roda JM. Update on the pathophysiology and management of syringomyelia unrelated to Chiari malformation [J]. Neurologia (Engl Ed), 2019, 34:318-325.

[4] Blegvad C, Grotenhuis JA, Juhler M. Syringomyelia: a practical, clinical concept for classification [J]. Acta Neurochir (Wien), 2014, 156:2127-2138.

[5] Cazes H, Carlino A. Plaisir de l'anatomie, plaisir du livre: "La Dissection des parties du corps humain" de Charles Estienne

(Paris, 1546)[J]. Cah Assoc Int Études Françaises, 2003, 55: 146-150.
[6] Yuan C, Guan J, Jian F. Rapid progression of acute cervical syringomyelia: a case report of delayed complications following spinal cord injury[J]. J Spinal Cord Med, 2022, 45:155-159.
[7] Leclerc A, Matveeff L, Emery E. Syringomyelia and hydromyelia: current understanding and neurosurgical management[J]. Rev Neurol (Paris), 2021, 177:498-507.
[8] Tosi U, Lara-Reyna J, Chae J, Sepanj R, Souweidane MM, Greenfield JP. Persistent syringomyelia after posterior fossa decompression for Chiari malformation[J]. World Neurosurg, 2020, 136:454-461.e1.
[9] Bruzek AK, Starr J, Garton HJL, Muraszko KM, Maher CO, Strahle JM. Syringomyelia in children with closed spinal dysraphism: long-term outcomes after surgical intervention[J]. J Neurosurg Pediatr, 2019.[Epub ahead of print]
[10] Hayashi T, Ueta T, Kubo M, Maeda T, Shiba K. Subarachnoid-subarachnoid bypass: a new surgical technique for posttraumatic syringomyelia[J]. J Neurosurg Spine, 2013, 18:382-387.
[11] Berliner J, Hemley S, Najafi E, Bilston L, Stoodley M, Lam M. Abnormalities in spinal cord ultrastructure in a rat model of post-traumatic syringomyelia[J]. Fluids Barriers CNS, 2020, 17:11.
[12] Mohrman AE, Farrag M, Huang H, Ossowski S, Haft S, Shriver LP, Leipzig ND. Spinal cord transcriptomic and metabolomic analysis after excitotoxic injection injury model of syringomyelia [J]. J Neurotrauma, 2017, 34:720-733.
[13] Berliner JA, Woodcock T, Najafi E, Hemley SJ, Lam M, Cheng S, Bilston LE, Stoodley MA. Effect of extradural constriction on CSF flow in rat spinal cord[J]. Fluids Barriers CNS, 2019, 16:7.
[14] Ma L, Yao Q, Zhang C, Li M, Cheng L, Jian F. Chronic extradural compression of spinal cord leads to syringomyelia in rat model[J]. Fluids Barriers CNS, 2020, 17:50.
[15] Guan J, Yuan C, Zhang C, Ma L, Yao Q, Cheng L, Liu Z, Wang K, Duan W, Wang X, Wang Z, Wu H, Chen Z, Jian F. A novel classification and its clinical significance in Chiar Ⅰ malformation with syringomyelia based on high-resolution MRI [J]. Eur Spine J, 2021, 30:1623-1634.
[16] Sakushima K, Tsuboi S, Yabe I, Hida K, Terae S, Uehara R, Nakano I, Sasaki H. Nationwide survey on the epidemiology of syringomyelia in Japan[J]. J Neurol Sci, 2012, 313:147-152.
[17] Wang J, Alotaibi NM, Samuel N, Ibrahim GM, Fallah A, Cusimano MD. Acquired Chiari malformation and syringomyelia secondary to space-occupying lesions: asystematicreview [J]. World Neurosurg, 2017, 98:800-808.e2.
[18] Ciappetta P, Signorelli F, Visocchi M. The role of arachnoid veils in Chiari malformation associated with syringomyelia[J]. Acta Neurochir Suppl, 2019, 125:97-99.
[19] Stoodley MA, Jones NR, Brown CJ. Evidence for rapid fluid flow from the subarachnoid space into the spinal cord central canal in the rat[J]. Brain Res, 1996, 707:155-164.
[20] Zhang Y, Zhang YP, Shields LB, Zheng Y, Xu XM, Whittemore SR, Shields CB. Cervical central canal occlusion induces noncommunicating syringomyelia[J]. Neurosurgery, 2012, 71: 126-137.
[21] Bertram CD, Heil M. A poroelastic fluid/structure: interactionmodel of cerebrospinal fluid dynamics in the cord with syringomyelia and adjacent subarachnoid-space stenosis [J]. J Biomech Eng, 2017, 139:011001-011010.
[22] Lee JY, Kim SW, Kim SP, Kim H, Cheon JE, Kim SK, Paek SH, Pang D, Wang KC. A rat model of chronic syringomyelia induced by epidural compression of the lumbar spinal cord[J]. J Neurosurg Spine, 2017, 27:458-467.
[23] Wong JH, Song X, Hemley SJ, Bilston LE, Cheng S, Stoodley MA. Direct-trauma model of posttraumatic syringomyelia with a computer-controlled motorized spinal cord impactor[J]. J Neurosurg Spine, 2016, 24:797-805.
[24] Andreollo NA, Santos EF, Araújo MR, Lopes LR. Rat′s age versus human′s age: what is the relationship[J]? Arq Bras Cir Dig, 2012, 25:49-51.
[25] Rey J, Sarntinoranont M. Pulsatile flow drivers in brain parenchyma and perivascular spaces: a resistance network model study[J]. Fluids Barriers CNS, 2018, 15:20.
[26] Heiss JD, Jarvis K, Smith RK, Eskioglu E, Gierthmuehlen M, Patronas NJ, Butman JA, Argersinger DP, Lonser RR, Oldfield EH. Origin of syrinx fluid in syringomyelia: aphysiologicalstudy [J]. Neurosurgery, 2019, 84:457-468.
[27] Liu S, Lam MA, Sial A, Hemley SJ, Bilston LE, Stoodley MA. Fluid outflow in the rat spinal cord: the role of perivascular and paravascular pathways[J]. Fluids Barriers CNS, 2018, 15:13.
[28] Brodbelt AR, Stoodley MA, Watling AM, Tu J, Jones NR. Fluid flow in an animal model of post-traumatic syringomyelia[J]. Eur Spine J, 2003, 12:300-306.
[29] Hemley SJ, Tu J, Stoodley MA. Role of the blood-spinal cord barrier in posttraumatic syringomyelia[J]. J Neurosurg Spine, 2009, 11:696-704.
[30] Tu J, Liao J, Stoodley MA, Cunningham AM. Reaction of endogenous progenitor cells in a rat model of posttraumatic syringomyelia[J]. J Neurosurg Spine, 2011, 14:573-582.
[31] Hemley SJ, Bilston LE, Cheng S, Stoodley MA. Aquaporin-4 expression and blood-spinal cord barrier permeability in canalicular syringomyelia[J]. J Neurosurg Spine, 2012, 17:602-612.
[32] Najafi E, Bilston LE, Song X, Bongers A, Stoodley MA, Cheng S, Hemley SJ. Longitudinal measurements of syrinx size in a rat model of posttraumatic syringomyelia[J]. J Neurosurg Spine, 2016, 24:941-948.
[33] Chakravarthy K, Kent AR, Raza A, Xing F, Kinfe TM. Burst spinal cord stimulation: review of preclinical studies and comments on clinical outcomes[J]. Neuromodulation, 2018, 21: 431-439.
[34] Wolfe KC, Poma R. Syringomyelia in the Cavalier King Charles spaniel (CKCS) dog[J]. Can Vet J, 2010, 51:95-102.
[35] Roser F, Ebner FH, Liebsch M, Dietz K, Tatagiba M. A new concept in the electrophysiological evaluation of syringomyelia [J]. J Neurosurg Spine, 2008, 8:517-523.
[36] Rusbridge C, Carruthers H, Dubé MP, Holmes M, Jeffery ND. Syringomyelia in cavalier King Charles spaniels: the relationship between syrinx dimensions and pain[J]. J Small Anim Pract, 2007, 48:432-436.
[37] Lara-Reyna J, Chae J, Tosi U, Souweidane MM, Uribe-Cardenas R, Greenfield JP. Syringomyelia resolution following Chiari surgery: anovelscale for communication and research [J]. Neurosurgery, 2020, 88:E60-66.
[38] Roach HI, Mehta G, Oreffo RO, Clarke NM, Cooper C. Temporal analysis of rat growth plates: cessation of growth with age despite presence of a physis[J]. J Histochem Cytochem, 2003, 51:373-383.
[39] Llorens-Bobadilla E, Chell JM, Le Merre P, Wu Y, Zamboni M, Bergenstråhle J, Stenudd M, Sopova E, Lundeberg J, Shupliakov O, Carlén M, Frisén J. A latent lineage potential in resident neural stem cells enables spinal cord repair[J]. Science, 2020, 370:eabb8795.
[40] Najafi E, Stoodley MA, Bilston LE, Hemley SJ. Inwardly rectifying potassium channel 4.1 expression in post-traumatic syringomyelia[J]. Neuroscience, 2016, 317:23-35.

（收稿日期：2022-08-21）
（本文编辑：柏钰）